Locomotion-based Hybrid Salp Swarm Algorithm for Parameter Estimation of Fuzzy Representation-based Photovoltaic Modules

Rizk M. Rizk-Allah and Aboul Ella Hassanien

***Abstract*—Identifying the parameters of photovoltaic (PV) modules is significant for their design and simulation. Because of the instabilities in the weather action and land surface of the earth, which cause errors in measuring, a novel fuzzy representation-based PV module is formulated and developed. In this paper, a novel locomotion-based hybrid salp swarm algorithm (LHSSA) is presented to identify the parameters of PV modules accurately and reliably. In the LHSSA, better leader salps based on particle swarm optimization (PSO) are incorporated to the traditional salp swarm algorithm (SSA) in a serialized scheme with the aim of providing more valuable information for the leader salps of the SSA. By this integration, the proposed LHSSA can escape the local optima as well as guide the seeking process to attain the promising region. The proposed LHSSA is investigated on different PV models, i.e., single-diode (SD), double-diode (DD), and PV module in crisp and fuzzy aspects. By comparing with different algorithms, the comprehensive results affirm that the LHSSA can achieve a highly competitive performance, especially on quality and reliability.**

***Index Terms*—Salp swarm algorithm (SSA), particle swarm optimization (PSO), photovoltaic (PV) model, hybridization.**

I. Introduction

BECAUSE of the rapid increase in air pollution caused by generating the power using fossil fuels, and greenhouse gas emissions, industrialized countries and governments need to rely on clean sources such as renewable energy sources. Presently, one of the most popular and promising renewable energy sources is solar energy (SE). SE is converted to electrical energy using photovoltaic (PV) systems [1]. PV components are easily deteriorated because they operate in harsh outdoor environments, significantly affecting the efficiency of the use of SE. As a result, the process of designing accurate models of PV systems becomes an important and challenging task due to the behavior evaluation of PV cells. Different mathematical models have been introduced to describe the nonlinear performance of PV systems [2], [3]. The most popular models are the single-diode (SD) and double-diode (DD) models [4], [5]. The accuracy of any model is mainly affected by adjusting the model parameters. However, these parameters have two problems: ① they are usually unavailable and change due to faults, volatile operation conditions, and aging; ② they have a certain degree of uncertainty due to the measurement process. Hence, the creation of an accurate scheme for parameter identification is a crucial and challenging task for the effective evaluation, simulation, and control of PV systems.

Some approaches based on deterministic techniques have been proposed for PV parameter identification based on deterministic techniques. Such approaches were developed based on the Newton approach [6], Lambert formulation [7], and so on [8]. However, some restrictions such as differentiability and convexity that lead to trapping in the local optima are present in the deterministic techniques.

The advent of metaheuristic approaches has provided promising alternative approaches for solving complex optimization tasks [9]-[12] and overcoming the limitations of the deterministic ones as well. Several approaches such as differential evolution (DE) have been introduced for the parameter identification problem [13]. In [14], artificial bee colony (ABC) was developed for identifying solar cell parameters, and in [15], a bacterial foraging approach (BFA) was used for parameter estimation of solar cells and other systems [16]-[18]. Salp swarm algorithm (SSA) is a new optimization approach that was proposed in [19] for solving optimization tasks. This algorithm is based on the behavior of salps, which form a chain through some leaders. Furthermore, through a rapid, coordinated change strategy, this behavior can achieve better convergence. However, as a new approach, SSA has some disadvantages: ① they are only guided by leaders, which leads to unsatisfactory outcomes; ② there is no strategy for the diversity and improving the best location with each generation, which may lead to trapping in the local optima. Besides, to the best of our knowledge, no attempts in the SSA literature have been employed to solve the parameter estimation of PV models.

Identifying the parameters of PV modules is significant for their design and simulation. Because of instabilities in the weather action and land surface of the earth, which cause errors in measuring, a novel fuzzy representation-

Manuscript received: January 15, 2019; accepted: August 16, 2019. Date of CrossCheck: August 16, 2019. Date of online publication: May 19, 2020.

R. M. Rizk-Allah is with the Faculty of Engineering, Menoufia University, Shebin El-Kom, Egypt, and he is also with Scientific Research Group in Egypt, Cario, Egypt (e-mail: rizk_masoud@yahoo.com).

A. E. Hassanien (corresponding author) is with the Faculty of Computers and Artificial Intelligence, Cairo University, Cairo, Egypt, and he is also with Scientific Research Group in Egypt, Cario, Egypt (e-mail: aboitcairo@gmail.com)

DOI: 10.35833/MPCE.2019.000028

based PV module is formulated and developed. In this sense, the PV modules are proposed in two aspects: the first aspect addresses crisp PV modules, while the second one concentrates on fuzzy modeling of PV modules in which the input data of terminal (output) voltage and solar cell terminal current are the fuzzy numbers. Through each fuzzy PV module, the terminal (output) voltage as well as the solar cell terminal current is characterized with the membership function. To effectively handle the crisp and fuzzy aspects of the PV modules, this paper hybridizes the SSA with the particle swarm optimization (PSO), in a scheme called the locomotion-based hybrid salp swarm algorithm (LHSSA), to effectively achieve robust identification of the parameters of the PV modules. In this approach, the SSA operates as an explorer tool for the solution vector while PSO is integrated to modify the locations of the leader salps. The performance of the proposed LHSSA is investigated and evaluated through different PV models. Comprehensive results affirm that the LHSSA exhibits superior performance compared with different algorithms, especially on the quality and reliability.

The main contributions of this paper are as follows.

1) An LHSSA-based opposition learning scheme is introduced to refine the quality of leaders.

2) A PSO algorithm-based leading method is incorporated to enhance exploitation capability and avoid trapping in the local optima.

3) Fuzzy representation-based PV models are introduced as a novel sight, and different level schemes are conducted.

4) The efficiency of the LHSSA is investigated by comprehensive experiments and the comparison on different PV models.

The remainder of this paper is organized as follows. Section II describes the formulation of the PV models. Section III provides some basics regarding the methodology. The proposed LHSSA is developed in Section IV. The results and the comparison of the different PV models are provided in Section V. Finally, the conclusions and potential for future study are exhibited in Section VI.

II. Problem Formulation

In practice, there are different PV models that describe the characteristics of the current-voltage performance of solar cells and PV modules. The formulation of these models associated with their objective functions is described in this section.

A. PV Models

1) SD Model

The SD model uses one diode that is parallel to a current source. The structure of this model includes a current source that is parallel to the circuit diode, one series resistor to represent the losses of load current, and a shunt resistor to represent the leakage current. The current of this cell is calculated using:

$$I_L = I_{ph} - I_d - I_{sh} \tag{1}$$

$$I_d = I_{sd}\left[\exp\left(\frac{q\left(V_L + R_S I_L\right)}{nkT}\right) - 1\right] \tag{2}$$

$$I_{sh} = \frac{V_L + R_S I_L}{R_{sh}} \tag{3}$$

where I_L is the terminal current of solar cell; I_{ph} is the photo-generated current; I_d is the diode current; I_{sh} is the shunt branch current; I_{sd} is the reverse saturation current; V_L is the terminal (output) voltage; R_{sh} and R_S are the shunt and series resistances, respectively; n is the diode ideal factor; q is the charge of an electron (1.60217646×10^{-19} C); k is the Boltzmann constant (1.3806503×10^{-23} J/K); and T is the temperature of the cell. According to (2) and (3), the terminal (output) current in (1) can be rewritten as:

$$I_L = I_{ph} - I_{sd}\left[\exp\left(\frac{q\left(V_L + R_S I_L\right)}{nkT}\right) - 1\right] - \frac{V_L + R_S I_L}{R_{sh}} \tag{4}$$

Although the SD contains five unknown parameters $(I_{ph}, I_{sd}, R_S, R_{sh}, n)$, [1] and [2] have shown that this optimization task has high multi-modal and noisy characteristics, thus this fact requires robust search strategies.

2) DD Model

The DD model considers two parallel diodes with a shunt resistance and current source. The terminal (output) current can be described as follows:

$$I_L = I_{ph} - I_{d1} - I_{d2} - I_{sh} = I_{ph} - I_{sd1}\left[\exp\left(\frac{q\left(V_L + R_S I_L\right)}{n_1 kT}\right) - 1\right] - I_{sd2}\left[\exp\left(\frac{q\left(V_L + R_S I_L\right)}{n_2 kT}\right) - 1\right] - \frac{V_L + R_S I_L}{R_{sh}} \tag{5}$$

where I_{d1} and I_{d2} are the first-diode and second-diode currents, respectively; I_{sd1} and I_{sd2} are the diffusion and saturation currents, respectively; and n_1 and n_2 are the ideal factors of diffusion and recombination diodes, respectively. In this case, seven unknown parameters $(I_{ph}, I_{sd1}, I_{sd2}, R_S, R_{sh}, n_1, n_2)$ need to be estimated to obtain the accurate performance of the solar cell.

3) PV Module Model

The PV module model is structured from several solar cells that are linked in series and/or in parallel. The output (terminal) current can be considered as follows:

$$\frac{I_L}{N_p} = I_{ph} - I_{sd}\left[\exp\left(\frac{q\left(V_L/N_S + R_S I_L/N_p\right)}{nkT}\right) - 1\right] - \frac{V_L/N_S + R_S I_L/N_p}{R_{sh}} \tag{6}$$

where N_S and N_p are the numbers of solar cells in series and parallel, respectively. This model contains five unknown parameters $(I_{ph}, I_{sd}, R_S, R_{sh}, n)$ that need to be identified.

B. Objective Function for PV Modules: Crisp Aspect

The main aim of the PV models is to minimize the difference between the experimental and estimated data. In this regard, the error function is represented and defined by (7) and (8) for the SD and DD, respectively.

$$\begin{cases} f_k(V_L, I_L, x) = I_{ph} - I_{sd}\left[\exp\left(\dfrac{q\left(V_L + R_S I_L\right)}{nkT}\right) - 1\right] - \dfrac{V_L + R_S I_L}{R_{sh}} - I_L \\ x = \left\{I_{ph}, I_{sd}, R_S, R_{sh}, n\right\} \end{cases} \tag{7}$$

$$\begin{cases} f_k(V_L, I_L, x) = I_{ph} - I_{sd1}\left[\exp\left(\dfrac{q\left(V_L + R_S I_L\right)}{n_1 kT}\right) - 1\right] - \\ \qquad I_{sd2}\left[\exp\left(\dfrac{q\left(V_L + R_S I_L\right)}{n_2 kT}\right) - 1\right] - \dfrac{V_L + R_S I_L}{R_{sh}} - I_L \\ x = \left\{I_{ph}, I_{sd1}, I_{sd2}, R_S, R_{sh}, n_1, n_2\right\} \end{cases} \tag{8}$$

where x is the solution set of the unknown parameters.

To objectively evaluate the performance of the proposed methodology, the objective function of the PV modules is formulated by quantifying the root mean square error (RMSE) as:

$$RMSE = \sqrt{\frac{1}{M}\sum_{k=1}^{M} f_k\left(V_L, I_L, x\right)^2} \tag{9}$$

$$\begin{cases} I_{ph,\min} \le I_{ph} \le I_{ph,\max} \\ R_{S,\min} \le R_S \le R_{S,\max} \\ R_{sh,\min} \le R_{sh} \le R_{sh,\max} \\ I_{sd,\min} \le I_{sd} \le I_{sd,\max} \\ I_{sd1,\min} \le I_{sd1} \le I_{sd1,\max} \\ I_{sd2,\min} \le I_{sd2} \le I_{sd2,\max} \\ n_{\min} \le n \le n_{\max} \\ n_{1,\min} \le n_1 \le n_{1,\max} \\ n_{2,\min} \le n_2 \le n_{2,\max} \end{cases} \tag{10}$$

where M is the number of experimental data; and the subscripts min and max represent the minimum and maximum values of related variables, respectively.

The main aim of the optimization process is to minimize the fitness function with respect to the bounds of the parameters. A smaller RMSE output implies a smaller deviation between the experimental and simulated data by the proposed algorithm.

C. Objective Function for PV Modules: Fuzzy Aspect

The electrical energy generated by PV modules involves many controlled parameters such as terminal (output) voltage and solar cell terminal current whose possible values are uncertain and ambiguous due to weather fluctuations or instabilities in the measuring process. Thus, the fuzzy model of the PV modules can be formulated as:

$$\begin{cases} \min \tilde{Z} = \sqrt{\dfrac{1}{M}\sum_{k=1}^{M} f_k\left(\tilde{V}_L, \tilde{I}_L, x\right)^2} \\ \text{s.t. (10)} \end{cases} \tag{11}$$

where $\tilde{Z}$ is the fuzzy objective form of RMSE; $\tilde{V}_L$ is the fuzzy terminal (output) voltage; and $\tilde{I}_L$ is the fuzzy solar cell terminal current. $\tilde{\delta} = \left(\tilde{V}_L, \tilde{I}_L\right)$ is the variable of the fuzzy parameters that are represented as fuzzy number. Each fuzzy number component of $\tilde{\delta}$ is associated by its own degree of membership function $\mu_{\tilde{\delta}}(\delta)$ [20].

Definition 1 (fuzzy number): the fuzzy number $\tilde{\delta}$ is a fuzzy subset of the real line R, which is associated with the membership function $\mu_{\tilde{\delta}}(\delta)$ that has the following features:

1) $\mu_{\tilde{\delta}}(\delta): R \to [0, 1]$ is continuous.

2) $\mu_{\tilde{\delta}}(\delta) = 0, \forall \delta \in (-\infty, \delta_1) \bigcap (\delta_3, +\infty)$.

3) Strictly increasing on $\delta \in [\delta_1, \delta_2]$.

4) $\mu_{\tilde{\delta}}(\delta) = 1$ for $\delta = \delta_2$.

5) Strictly decreasing on $\delta \in [\delta_2, \delta_3]$.

Therefore, each measured value of the terminal voltage and solar cell terminal current can be represented by a certain "grade of membership" that ranges from grade 0 to 1, where 0 and 1 indicate the lowest and highest grades of membership, respectively. Thus, each fuzzy parameter is expressed by a given interval of real numbers, associated with grades of membership between 0 and 1.

Definition 2 (α-level set): the α-level set (α-cut) of the fuzzy numbers $\tilde{\delta}$ is represented by the ordinary set $L_\alpha\left(\tilde{\delta}\right)$ that contains the values of δ when the degree of membership functions exceeds a certain level α, $\alpha \in [0, 1]$.

$$L_\alpha\left(\tilde{\delta}\right) = \left\{\delta | \mu_{\tilde{\alpha}}(\delta) \ge \alpha\right\} \tag{12}$$

The fuzzy representation shown in Fig. 1 has been extracted according to expert suggestions or from observing weather fluctuations or instabilities in the measuring process. Based on the α-cut concept of the fuzzy numbers, the problem with the fuzzy parameters aspect can be converted into a crisp aspect. The membership function $\mu_{\tilde{\delta}}(\delta)$ which defines the fuzzy parameter $\tilde{\delta}$ is formulated as:

$$\mu_{\tilde{\delta}}(\delta) = \begin{cases} 1 & \delta = \tilde{\delta} \\ \dfrac{20\delta}{\tilde{\delta}} - 19 & 0.95\tilde{\delta} \le \delta < \tilde{\delta} \\ 21 - \dfrac{20\delta}{\tilde{\delta}} & \tilde{\delta} < \delta \le 1.05\tilde{\delta} \\ 0 & \delta < 0.95\tilde{\delta} \text{ or } \delta > 1.05\tilde{\delta} \end{cases} \tag{13}$$

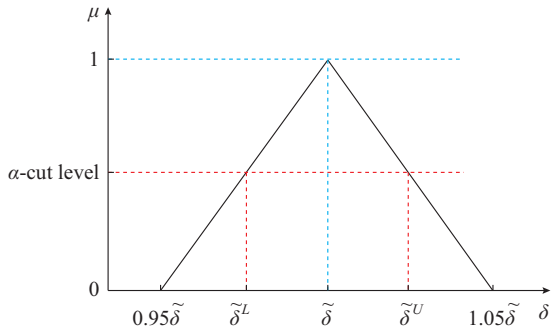

Fig. 1. Fuzzy numbers for PV modules.

According to the membership function and the concept of the α-cut level, the fuzzy parameter is transformed to a crisp scheme through two end points which are induced by the α-cut level, and they represent the upper and lower bounds for the crisp parameter, as shown in Fig. 1, where $\tilde{\delta}^L$ and $\tilde{\delta}^U$ are the lower and upper bounds induced by α-cut for parameter δ, respectively. Thus, the optimization task of the PV modules can be converted to a non-fuzzy (crisp) form as:

$$\begin{cases} \min Z = \sqrt{\dfrac{1}{M}\sum_{k=1}^{M} f_k\left(V_{Lk}, I_{Lk}, x\right)^2} \\ \text{s.t. (10)} \\ \quad \tilde{V}_{Lk}^{L} \le V_{Lk} \le \tilde{V}_{Lk}^{U} \quad k = 1, 2, ..., M \\ \quad \tilde{I}_{Lk}^{L} \le I_{Lk} \le \tilde{I}_{Lk}^{U} \quad k = 1, 2, ..., M \end{cases} \tag{14}$$

where superscripts L and U represent the lower and upper bounds of related variables, respectively.

Definition 3 (α-global minimum): x^* is defined as the α-global minimum to the problem (14) if and only if $\forall x \in \Psi, \delta \in L_\alpha\left(\tilde{\delta}\right): Z\left(x^*, \delta^*\right) \le Z\left(x, \delta\right)$, where Ψ is the feasible region of the search space and δ^* is the α-level optimal parameter.

D. Overview of SSA

The SSA is a meta-heuristic optimization algorithm presented in [19]. It mimics the natural behavior of salps living in the deep parts of oceans. Salps are a type of Salpidae and look like jelly fish with a transparent body. Salps have an intelligent behavior during their navigation and foraging as a salp chain. In this context, the SSA is a recent type of swarm algorithm developed to model the salp chain [19]. In the salp chain, the salp population is split into two categories: the leader salp which is the first salp in the chain, and the follower salps that follow the leader salp while reaching for the food source. The position set of each salp in the search space is $x^i = \{x_1^i, x_2^i, ..., x_d^i\}, i = 1, 2, ..., N$, where N is the number of salps. Thus, the leader salp updates its position as:

$$x_j^1 = \begin{cases} F_j + h_1\left[\left(ub_j - lb_j\right)h_2 + lb_j\right] & h_3 \ge 0.5 \\ F_j - h_1\left[\left(ub_j - lb_j\right)h_2 + lb_j\right] & h_3 < 0.5 \end{cases} \tag{15}$$

where ub_j and lb_j are the upper and lower bounds in the j^{th} dimension, respectively; F_j is the position of the target source in the j^{th} dimension; and h_1, h_2, and h_3 are the algorithm parameters. The first parameter h_1, which is responsible for balancing the exploration and the exploitation mechanisms, is the most important parameter, and is defined as:

$$h_1 = 2\mathrm{e}^{-\left(\frac{4t}{L}\right)^2} \tag{16}$$

where t and L are the current iteration and maximum iteration, respectively. h_2 and h_3 are random numbers between 0 and 1 whose values are uniformly generated. Furthermore, each follower salp updates its position based on Newton's law of motion using the following equation.

$$x_j^i = \frac{1}{2}\left(x_j^i + x_j^{i-1}\right) \quad 2 \ge i > N \tag{17}$$

where x_j^i is the position of the i^{th} follower salp in the j^{th} dimension.

E. PSO

PSO is a population-based algorithm introduced in [21]. It is inspired by the cooperative behavior of some birds, fishes, and insects. In PSO, each particle improves its position by considering its best personal and global positions. The position of each particle x_i is updated as:

$$v_i^{t+1} = wv_i^t + c_1 r_1\left(p_i^t - x_i^t\right) + c_2 r_2\left(g_i^t - x_i^t\right) \tag{18}$$

$$x_i^{t+1} = x_i^t + v_i^{t+1} \tag{19}$$

where x_i^t and v_i^t are the current position of the i^{th} particle and its velocity at iteration t, respectively; p_i^t is the best position of the i^{th} particle; g_i^t is the best solution among all particles; c_1 and c_2 are the cognitive and social parameters, respectively; w is the inertia weight; and r_1 and r_2 are the random numbers between 0 and 1.

III. Proposed LHSSA Algorithm

The motivation behind developing the LHSSA is to achieve two features: ① improving the locomotion of the leader salps by memorizing the track of the leader; ② enhancing the seeking process using the hybridization-based PSO.

A. Locomotion-based Internal Memory

An internal memory is incorporated for the leader salps to keep track of their positions. During each iteration, the best agents between the salps and particles are saved and denoted by personal leaders $S_{B,leader}$ and the global leader is denoted by $S_{G,leader}$.

B. Hybridization-based Iteration

Hybridization-based iteration is a straightforward approach for executing two algorithms iteratively through a certain sequence to enhance optimization performance [22]. Here, SSA works as an explorer using (14), while PSO is responsible for exploiting the previous leader salps to obtain more refined leaders. Thus, the modified position and velocity equations of PSO are defined as:

$$v_i^{t+1} = wv_i^t + c_1 r_1\left(S_{B,leader,i}^t - x_i^t\right) + c_2 r_2\left(S_{G,leader}^t - x_i^t\right) \tag{20}$$

$$x_i^{t+1} = x_i^t + v_i^{t+1} \tag{21}$$

where $S_{B,leader,i}^t$ is the personal best for the i^{th} particle of PSO; and $S_{G,leader}^t$ is the global best of the swarm in the iteration t of the PSO.

C. Experience-based Opposition Learning Scheme

The opposition learning scheme based on the behavior of follower salps is developed to improve swarm diversity with the aim of increasing exploration ability. To be specific, for each follower salp, the opposition solution is defined as in (22).

$$x'_{i,j,t} = \begin{cases} rand\left(LB_j + UB_j\right) - x_{i,j,t} & x'_{i,j,t} \in \left(B_j, UB_j\right) \\ rand\left(LB_j, UB_j\right) & \text{otherwise} \end{cases} \tag{22}$$

where $x'_{i,j,t}$ is the j^{th} element of the i^{th} opposition solution set on the t^{th} iteration; and LB_j and UB_j are the dynamic bounds of the j^{th} variable defined as:

$$\begin{cases} LB_j = \min\left(x_{i,j,t}\right) \\ UB_j = \max\left(x_{i,j,t}\right) \end{cases} \tag{23}$$

LB_j and UB_j are updated every 50 generations and if the obtained solution does not lie within the bounds, a random solution is generated. The flow chart of the proposed scheme is given in Fig. 2.

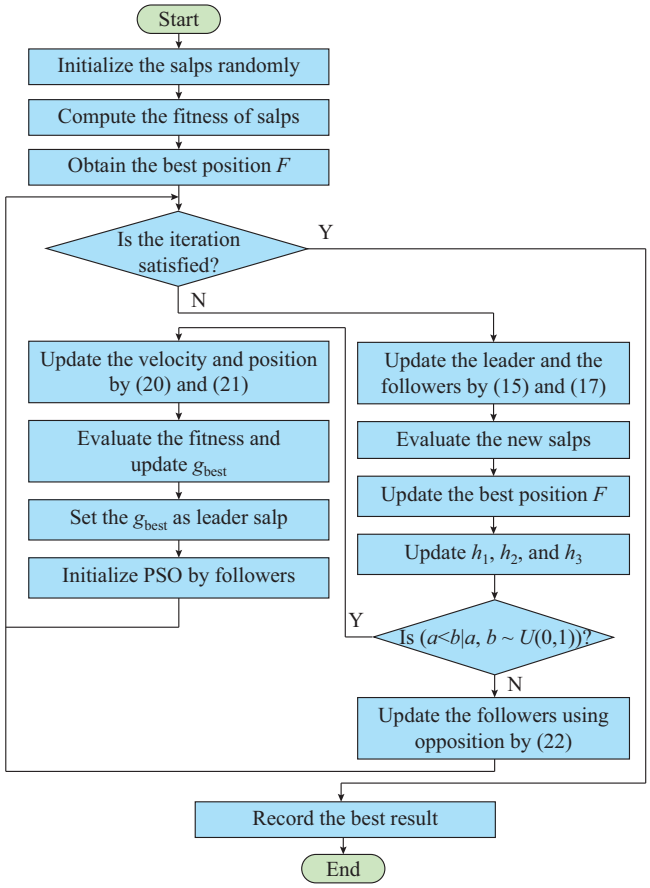

Fig. 2. Flow chart of proposed LHSSA.

IV. Experimental Results and Analysis

The performance of LHSSA is investigated to identify the parameters of different PV models such as the SD, DD, and PV module. Thus, the benchmark data set for the solar cells and solar module is utilized [23]. To guarantee accurate comparison, the bounds for the parameters are given in Table I [23]. In this context, the superior performance of the proposed LHSSA is validated by comparing with other well-established algorithms [24] such as PSO, fire fly algorithm (FFA), grey wolf algorithm (GWO), dragonfly algorithm (DA), and standard SSA. For fair comparisons, the same maximum number of iterations in each run with 20 independent runs for every problem is adopted in the comparative algorithms. Further, the parameter configurations of the compared algorithms are listed in Table II and are suggested as in [24].

TABLE I
Parameters Range for SD, DD, and PV Module

Model	Bound	I_{ph} (A)	I_{sd}, I_{sd1}, I_{sd2} (μA)	R_S (Ω)	R_{sh} (Ω)	n, n_1, n_2
SD	Lower	0	0	0.0	0	1
	Upper	1	1	0.5	100	2
DD	Lower	0	0	0.0	0	1
	Upper	1	1	0.5	100	2
PV module	Lower	0	0	0.0	0	1
	Upper	2	50	2.0	2000	50

TABLE II
Parameter Configurations for Comparative Algorithms

Parameter	Algorithm
Population size $PS=20$, acceleration coefficients $c_1=c_2=2$, inertia weight w: 0.2-0.9	PSO
$PS=20$, initial attractiveness $\beta_0=1$, randomization parameter $\alpha=0.2$, absorption coefficient $\gamma=1$	FFA
$PS=20$, $a\in[0,2], A=2ar_2-a, C=2r_1, r_1, r_2 \sim U(0,1)$, U represents a uniform distribution	GWO
$PS=20$, w: 0.2-0.9, separation $s=0.1$, alignment $a=0.1$, cohesion $c=0.7$, food $f=1$, enemy $e=1$	DA
$PS=20$, $h_1\in[0,2]$, $h_2, h_3\in[0,1]$	SSA
$PS=20$, acceleration coefficients: $c_1=c_2=2$, inertia weight w: 0.2-0.9, $h_1\in[0,2]$, $h_2, h_3\in[0,1]$	LHSSA

A. Results of SD Model

In this section, the comparison results of the SD model including the extracted parameters and RMSE are shown in Table III, where the best RMSE value among all comparative algorithms is highlighted in boldface.

The results of all the comparative algorithms and the results taken from [23] are listed in Table III, where the meaning of the abbreviations can be found in [23]. Regarding Table III, it can be observed that the proposed LHSSA gives the lowest RMSE value (0.98602 mA) compared with the other comparative algorithms. Additionally, to further emphasize the quality of the obtained results, the best extracted parameters of the LHSSA are employed to replot the *I-V* and *P-V* characteristic curves as depicted in Fig. 3. The depicted curves show that the calculated data acquired by the LHSSA highly coincides with the measured one based on the voltage range. Additionally, the individual absolute error (IAE) is introduced as a quality index to determine the absolute difference between the experiment data I^{tm} and the simulated one I^{te} as in Table IV. The obtained values of the IAE are less than 1.62×10^{-3} and the total sum is 2.58×10^{-5}, which affirms the accuracy of the parameters estimated by the LHSSA.

B. Results of DD Model

The parameters of the DD model associated with the RMSE of the different methods are recorded in Table V. The results of the compared algorithms are also presented in Table V. It is obvious that the proposed LHSSA outperforms the comparative algorithms because it provides the best RMSE value (0.98249 mA). The characteristic curves for *I-V* and *P-V* of the measured data and the one estimated by the LHSSA are depicted in Fig. 4, whereas the IAE values are given in Table VI. Figure 4 shows that the data estimated by the LHSSA are in good congruence with the measured data. From Table VI, the sum of errors is 3.84×10^{-6} and all the IAE values are smaller than 1.239×10^{-3}, indicating the high accuracy of the identified parameters.

C. Results of PV Module Model

In this model, five parameters are estimated and the RMSE values are obtained and reported in Table VII.

TABLE III
COMPARISONS WITH VARIOUS ALGORITHMS FOR SD MODEL

Algorithm	R_s (Ω)	R_{sh} (Ω)	I_{ph} (A)	I_{sd} (μA)	n	RMSE (mA)
Proposed LHSSA	0.03640	53.7185	0.7607	0.32300	1.48170	**0.98602**
PSO	2.22040×10^{-16}	1.1489	0.8368	2.22000×10^{-8}	1.00000	19.58100
FFA	0.01540	47.0033	0.5697	3.09000	1.89920	141.63000
GWO	0.02970	32.6211	0.7652	1.10700	1.61860	222.86000
DA	2.22040×10^{-16}	1.1489	0.8368	2.22000×10^{-8}	1.00000	222.86000
SSA	4.73800×10^{-4}	5.6237	0.7443	11.02000	1.98690	39.90600
IJAYA	0.03640	53.7595	0.7608	0.32280	1.48110	0.98603
JAYA	0.03640	54.9298	0.7608	0.32810	1.48280	0.98946
GOTLBO	0.03630	53.3664	0.7608	0.32970	1.48330	0.98856
LETLBO	0.03630	53.7429	0.7608	0.32597	1.48210	0.98738
LBSA	0.03640	54.1083	0.7609	0.32583	1.48200	0.99125
CLPSO	0.03610	54.1965	0.7608	0.34302	1.48730	0.99633
BLPSO	0.03590	60.2845	0.7607	0.36620	1.49390	1.02720
DE/BBO	0.03640	55.2627	0.7605	0.32477	1.48170	0.99922
CMM-DE/BBO	0.03640	53.8753	0.7608	0.32384	1.48140	0.98605
IADE	0.03621	54.7643	0.7607	0.33613	1.48520	0.98900
IGHS	0.03610	53.2845	0.7608	0.34350	1.48740	0.99306
ABSO	0.03659	52.2903	0.7608	0.30623	1.47878	0.99124

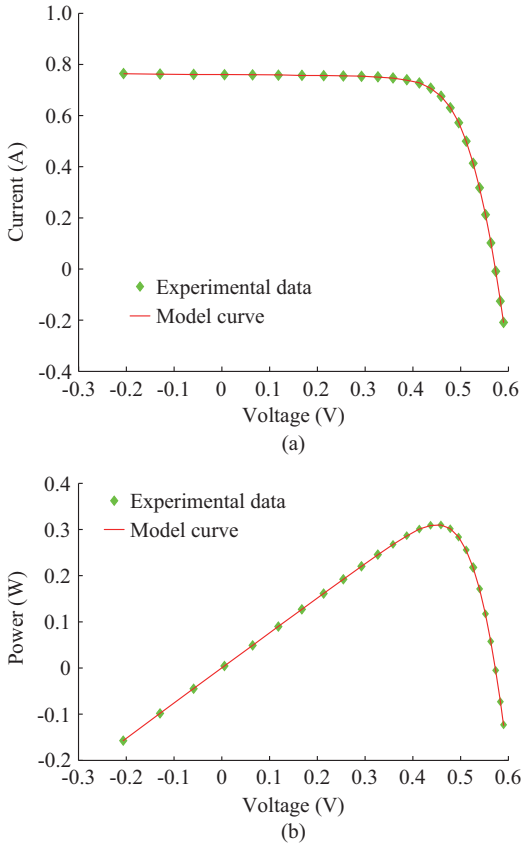

Fig. 3. Comparison between experimental and simulated data obtained by LHSSA for SD model. (a) *I-V* characteristics. (b) *P-V* characteristics.

The results of the proposed LHSSA are compared with different algorithms, some of which are taken from literature for comparison [23]. The overall IAE values are given in Table VIII.

TABLE IV
IAE OF LHSSA FOR EACH MEASUREMENT ON SD MODEL

Item	Measured voltage (V)	Measured current (A)	Calculated current (A)	IAE
1	−0.2057	0.7640	0.7640	−0.0000872
2	−0.1291	0.7620	0.7626	−0.0006600
3	−0.0588	0.7605	0.7613	−0.0008500
4	0.0057	0.7605	0.7601	0.0003500
5	0.0646	0.7600	0.7590	0.0009500
6	0.1185	0.7590	0.7580	0.0009600
7	0.1678	0.7570	0.7571	−0.0000911
8	0.2132	0.7570	0.7561	0.0008600
9	0.2545	0.7555	0.7551	0.0004100
10	0.2924	0.7540	0.7536	0.0003400
11	0.3269	0.7505	0.7513	−0.0008900
12	0.3585	0.7465	0.7473	−0.0008500
13	0.3873	0.7385	0.7401	−0.0016200
14	0.4137	0.7280	0.7273	0.0006200
15	0.4373	0.7065	0.7069	−0.0004700
16	0.4590	0.6755	0.6752	0.0002200
17	0.4784	0.6320	0.6307	0.0012400
18	0.4960	0.5730	0.5719	0.0010700
19	0.5119	0.4990	0.4996	−0.0006100
20	0.5265	0.4130	0.4136	−0.0006500
21	0.5398	0.3165	0.3175	−0.0010100
22	0.5521	0.2120	0.2121	−0.0001500
23	0.5633	0.1035	0.1022	0.0012500
24	0.5736	−0.0100	−0.0087	−0.0012800
25	0.5833	−0.1230	−0.1255	0.0025100
26	0.5900	−0.2100	−0.2084	−0.0015200

TABLE V
COMPARISONS WITH VARIOUS ALGORITHMS FOR DD MODEL

Algorithm	R_s (Ω)	R_{sh} (Ω)	I_{ph} (A)	I_{sd1} (μA)	I_{sd2} (μA)	n_1	n_2	RMSE (mA)
Proposed LHSSA	0.036740	55.4824	0.76080	0.7473	0.2259	2.0000	1.4515	0.98249
PSO	2.220400×10^{-16}	1.1487	0.83680	2.2204×10^{-10}	2.2204×10^{-10}	1.0000	1.0000	222.86000
FFA	2.220400×10^{-16}	1.1904	0.86410	2.2204×10^{-10}	2.2204×10^{-10}	1.8384	1.3378	226.05000
GWO	0.048295	22.6562	0.76170	8.3152×10^{-3}	2.4189×10^{-10}	1.1862	1.5192	6.61280
DA	2.220400×10^{-16}	1.1489	0.83680	2.2204×10^{-10}	2.2204×10^{-10}	1.0000	1.1676	222.86000
SSA	5.613300×10^{-4}	1.9814	0.83910	2.2204×10^{-10}	3.9483	1.9963	1.8427	82.60300
IJAYA	0.037600	77.8519	0.76010	0.0050	0.7509	1.2186	1.6247	0.98293
JAYA	0.036400	52.6575	0.76070	0.0061	0.3151	1.8436	1.4788	0.98934
GOTLBO	0.036500	53.4058	0.76080	0.1389	0.2621	1.7254	1.4658	0.98742
LETLBO	0.036500	54.3021	0.76080	0.1739	0.2266	1.6585	1.4578	0.98565
LBSA	0.036500	56.0524	0.76070	0.2487	0.2744	1.8817	1.4682	0.98751
CLPSO	0.036700	57.9422	0.76070	0.2584	0.3862	1.4625	1.9435	0.99894
BLPSO	0.036600	61.1345	0.76080	0.2719	0.4351	1.4674	1.9662	1.06280
DE/BBO	0.038500	58.4018	0.76060	0.0012	0.3722	1.8791	1.4956	1.02550
CMM-DE/BBO	0.036000	57.9882	0.76070	0.3537	0.0256	1.4907	1.8835	1.00880
IGHS	0.036900	53.8368	0.76080	0.9731	0.1679	1.9213	1.4281	0.98635
ABSO	0.036600	54.6219	0.76077	0.2671	0.3819	1.4651	1.9815	0.98344

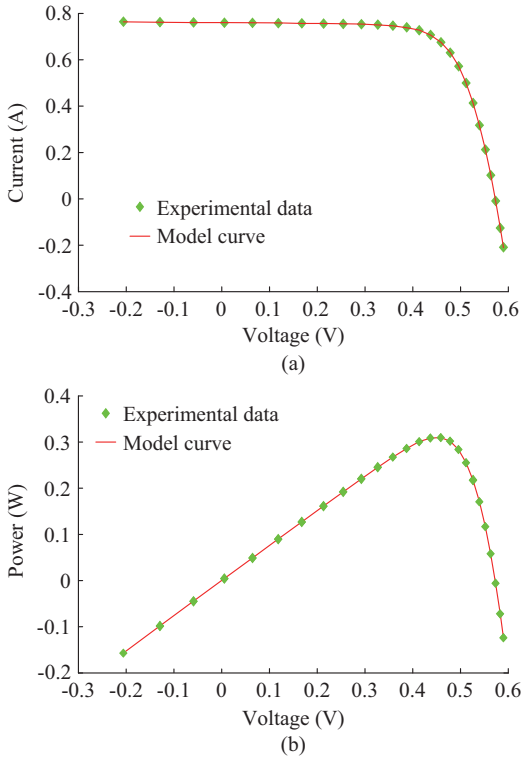

Fig. 4. Comparison between experimental and simulated data obtained by LHSSA for DD model. (a) *I-V* characteristics. (b) *P-V* characteristics.

It is clear that the proposed LHSSA outperforms the other algorithms as it gives the best RMSE value (2.42507×10^{-3}) among all the compared algorithms. The comparison shows that the LHSSA performs well. Due to space limitations, the *I-V* and *P-V* characteristics are not depicted. The obtained IAE values are all smaller than 4.837×10^{-3} and the total sum of error is 4.3172×10^{-5}. The parameters with high accuracy are achieved again by the LHSSA.

TABLE VI
IAE OF LHSSA FOR EACH MEASUREMENT ON DD MODEL

Item	Measured voltage (V)	Measured current (A)	Calculated current (A)	IAE
1	–0.2057	0.7640	0.7639	0.0000165
2	–0.1291	0.7620	0.7626	–0.0006200
3	–0.0588	0.7605	0.7613	–0.0008400
4	0.0057	0.7605	0.7602	0.0003300
5	0.0646	0.7600	0.7591	0.0008900
6	0.1185	0.7590	0.7581	0.0008800
7	0.1678	0.7570	0.7572	–0.0001900
8	0.2132	0.7570	0.7562	0.0007600
9	0.2545	0.7555	0.7552	0.0003200
10	0.2924	0.7540	0.7537	0.0002800
11	0.3269	0.7505	0.7514	–0.0009100
12	0.3585	0.7465	0.7473	–0.0008000
13	0.3873	0.7385	0.7400	–0.0015100
14	0.4137	0.7280	0.7272	0.0007500
15	0.4373	0.7065	0.7069	–0.0003500
16	0.4590	0.6755	0.6752	0.0002900
17	0.4784	0.6320	0.6308	0.0012400
18	0.4960	0.5730	0.5720	0.0010100
19	0.5119	0.4990	0.4998	–0.0007100
20	0.5265	0.4130	0.4137	–0.0007300
21	0.5398	0.3165	0.3175	–0.0010500
22	0.5521	0.2120	0.2121	–0.0001200
23	0.5633	0.1035	0.1022	0.0013400
24	0.5736	–0.0100	–0.0088	–0.0012100
25	0.5833	–0.1230	–0.1255	0.0025400
26	0.5900	–0.2100	–0.2084	–0.0016300

TABLE VII
RESULTS AMONG COMPARATIVE TECHNIQUES ON PV MODULE

Algorithm	R_s (Ω)	R_{sh} (Ω)	I_{ph} (A)	I_{sd} (μA)	n	RMSE (mA)
Proposed LHSSA	0.0334	27.2773	1.0305	3.4822	1.3517	2.4250
PSO	0	2000.0000	1.1741	3046.3000	2.8761	77.5850
FFA	0	586.7000	1.4650	226590.0000	9.1139	220.4100
GWO	0.0005	1064.5000	1.0467	680.5200	2.3241	23.5320
DA	0	2000.0000	1.0484	765.8700	2.3616	23.8810
SSA	0	1931.5000	1.3032	54173.0000	5.3692	144.9300
IJAYA	1.2016	977.3700	1.0305	3.4703	48.6298	2.4251
JAYA	1.2014	1022.5000	1.0302	3.4931	48.6531	2.4278
GOTLBO	1.1995	969.9300	1.0307	3.5124	48.6766	2.4266
LETLBO	1.2015	974.6100	1.0306	3.4705	48.6301	2.4251
LBSA	1.2010	987.7800	1.0305	3.4901	48.6513	2.4252
CLPSO	1.1978	1017.0000	1.0304	3.6131	48.7847	2.4281
BLPSO	1.2002	992.7900	1.0305	3.5176	48.6815	2.4252
DE/BBO	1.1969	1015.1000	1.0303	3.6172	48.7894	2.4283
CMM-DE	1.2013	981.9800	1.0305	3.4823	48.6428	2.4251
PS	1.2053	714.2800	1.0313	3.1756	48.2889	11.8000
SA	1.1989	833.3300	1.0331	3.6642	48.8211	2.7000

TABLE VIII
IAE OF LHSSA FOR EACH MEASUREMENT ON PV MODULE

Item	Measured voltage (V)	Measured current (A)	Calculated current (A)	IAE
1	0.1248	1.0315	1.02912	0.0023800
2	1.8093	1.0300	1.02738	0.0026200
3	3.3511	1.0260	1.02574	0.0002600
4	4.7622	1.0220	1.02411	–0.0021100
5	6.0538	1.0180	1.02229	–0.0042900
6	7.2364	1.0155	1.01993	–0.0044300
7	8.3189	1.0140	1.01636	–0.0023600
8	9.3097	1.0100	1.01049	–0.0005000
9	10.2163	1.0035	1.00063	0.0028700
10	11.0449	0.9880	0.98455	0.0034500
11	11.8018	0.9630	0.95952	0.0034800
12	12.4929	0.9255	0.92284	0.0026600
13	13.1231	0.8725	0.87260	–0.0001000
14	13.6983	0.8075	0.80728	0.0002200
15	14.2221	0.7265	0.72834	–0.0018400
16	14.6995	0.6345	0.63714	–0.0026400
17	15.1346	0.5345	0.53622	–0.0017100
18	15.5311	0.4275	0.42951	–0.0020100
19	15.8929	0.3185	0.31877	–0.0002700
20	16.2229	0.2085	0.20739	0.0011100
21	16.5241	0.1010	0.09616	0.0048400
22	16.7987	–0.0080	–0.00833	0.0003300
23	17.0499	–0.1110	–0.11095	–0.0000538
24	17.2793	–0.2090	–0.20926	0.0002600
25	17.4885	–0.3030	–0.30088	–0.0021200

D. Statistical Measures and Convergence Behavior

In this subsection, statistical measures are calculated for the proposed and comparative algorithms over 20 independent runs and are recorded in Table IX. These measures include the mean RMSE that quantifies the average accuracy and also confirms the stability of the algorithm runs, and St. dev that represents the standard deviation of the RMSE values that defines the reliability of the parameter estimation. For each model, the overall best RMSE values among the comparative algorithms are highlighted in boldface. Table IX demonstrates that the proposed LHSSA performs much better than all the other comparative algorithms for all the models in terms of reliability and accuracy. In this regard, the convergence curves for the comparative algorithms are depicted in Fig. 5 and the box-plot representations are used to show the distribution of the results obtained by those algorithms over 20 independent runs, as shown in Fig. 6. It is noted that the LHSSA has a faster convergence rate than the other algorithms in all models.

E. Study of Fuzzy Representation

The imprecise descriptions of the solar cell models are often caused by weather fluctuations or instabilities in the measuring process. Thus, new insight from the operating point of view is presented by incorporating this impreciseness using the fuzzy concept in the solar cell models. The fuzzy number representation is illustrated in Section II. Additionally, the fuzzified value is transformed into a crisp value based on the α-cut level, using upper and lower bound values.

A searching process is carried out to identify the optimal values for the parameters in terms of the α level. This strategy is investigated on the SD, DD and PV module models at different levels, but the results are reported for $\alpha = 0.8$ only due to space limitation. The estimated parameters are recorded in Tables X-XII. The convergence curves and box plot are demonstrated for the DD model only due to space limitation in Figs. 7 and 8, respectively. The statistical measures for these models are also listed in Table XIII.

F. Effects of α-level Schemes on RMSE

In order to clear the effects of the α-level schemes on RMSE, three cases are considered ($\alpha = 1, \alpha = 0.8, \alpha = 0.4$) as in Fig. 9, where $\alpha = 1$ represents the crisp case. Based on the obtained results, the RMSE is affected by the vagueness aspect induced by the α-level cut. Finally, we hope that this paper will inspire researchers in studying the uncertainty aspect of different solar cell performances, which is caused by various factors such as shading, weather changes and so on.

V. CONCLUSION

In this paper, a novel LHSSA is presented to accurately estimate the parameters of PV models. In the LHSSA, the standard SSA is conducted to search globally and explore the different areas in the search space. Afterwards, PSO is employed to guide the SSA leaders with the aim of eliciting the promising area. Additionally, a learning scheme based on the follower behavior is introduced with the aim of improving the population diversity. In this regard, the SSA emphasizes on the diversification while PSO focuses on the intensification.

TABLE IX
STATISTICAL MEASURES OF DIFFERENT TECHNIQUES FOR THREE MODELS

Model	Algorithm	RMSE (mA)			
		Min	Mean	Max	St.dev
SD	LHSSA	**0.98602**	**0.98602**	**0.98602**	**6.269700×10^{-10}**
	PSO	19.58100	212.69000	222.86000	45.454000
	FFA	141.64000	225.21000	241.84000	20.333000
	GWO	222.86000	222.86000	222.87000	4.254900×10^{-3}
	DA	222.86000	222.86000	222.86000	1.042400×10^{-13}
	SSA	39.90600	121.35000	222.86000	44.665000
	IJAYA	0.98603	0.99204	1.06220	1.403300×10^{-2}
	JAYA	0.98946	1.16170	1.47830	0.187960
	GOTLBO	0.98856	1.04500	1.20670	0.502180
	LETLBO	0.98738	1.03330	1.15930	0.469460×10^{-2}
	LBSA	0.99125	1.14660	1.48620	0.134820
	CLPSO	0.99633	1.05810	1.31960	7.485400×10^{-2}
	BLPSO	1.02720	1.31390	1.79280	0.211660
	DE/BBO	0.99922	1.29480	2.22580	0.250740
	CMM-DE/BBO	0.98605	1.04860	1.34750	8.167900×10^{-2}
DD	LHSSA	**0.98249**	**0.98337**	**0.98602**	**1.494500×10^{-3}**
	PSO	222.86000	230.57000	299.95000	24.378000
	FFA	226.06000	244.84000	266.29000	11.980500
	GWO	6.61290	159.45000	222.87000	102.160000
	DA	222.86000	222.86000	222.86000	1.072200×10^{-4}
	SSA	82.60300	147.24000	165.79000	24.236000
	IJAYA	0.98293	1.02690	1.40550	0.098325
	JAYA	0.98934	1.17670	1.47930	0.193560
	GOTLBO	0.98742	1.14750	1.39470	0.113300
	LETLBO	0.98565	1.08690	1.48700	0.153600
	LBSA	0.98751	1.25450	1.73430	0.222360
	CLPSO	0.99894	1.14580	1.54940	0.143670
	BLPSO	1.06280	1.48210	1.74110	0.177890
	DE/BBO	1.02550	1.55710	2.40420	0.362970
	CMM-DE/BBO	1.00880	1.54870	2.05890	0.294130
PV module	LHSSA	**2.42500**	**2.42500**	**2.42500**	**3.525700×10^{-9}**
	PSO	77.58500	202.35000	274.25000	87.493000
	FFA	220.41000	242.59000	261.92000	15.209000
	GWO	23.53200	99.18200	274.29000	120.820000
	DA	23.88100	213.11000	274.25000	96.186000
	SSA	144.93000	186.23000	246.43000	37.828000
	IJAYA	2.42510	2.42890	2.43930	3.775500×10^{-3}
	JAYA	2.42780	2.45370	2.59590	3.456300×10^{-2}
	GOTLBO	2.42660	2.47540	2.56380	2.938800×10^{-2}
	LETLBO	2.42510	2.44070	2.58210	2.949000×10^{-2}
	LBSA	2.42520	2.46740	2.53440	2.910900×10^{-2}
	CLPSO	2.42810	2.45490	2.54330	2.581000×10^{-2}
	BLPSO	2.42520	2.43790	2.48830	1.372400×10^{-2}
	DE/BBO	2.42830	2.46160	2.52560	2.925100×10^{-2}
	CMM-DE/BBO	2.42510	2.42520	2.42680	3.554800×10^{-4}

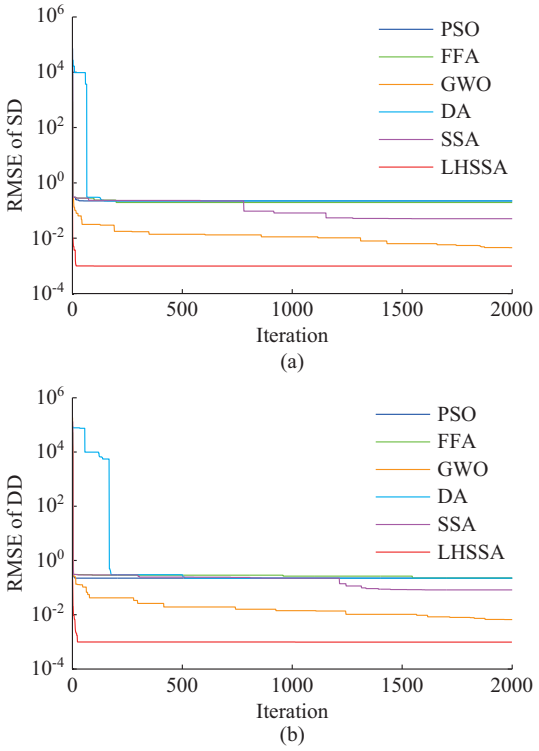

Fig. 5. Convergence curves for two models. (a) SD model. (b) DD model.

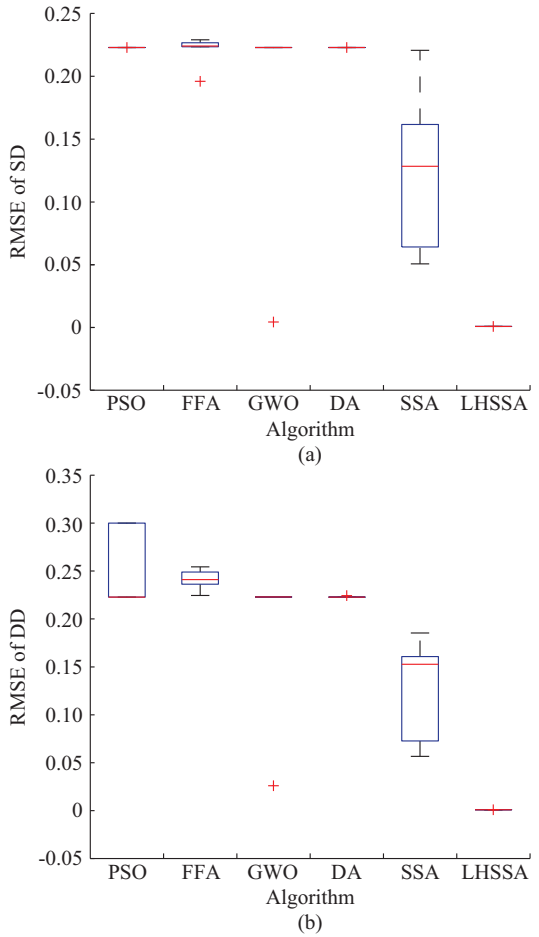

Fig. 6. Boxplot representations of RMSE for SD model and DD model. (a) SD model. (b) DD model.

TABLE X
ESTIMATED PARAMETERS IN FUZZY ENVIRONMENT (SD MODEL) WHEN $\alpha = 0.8$

Algorithm	R_s (Ω)	R_{sh} (Ω)	I_{ph} (A)	I_{sd} (μA)	n	RMSE (mA)
PSO	2.2204×10^{-16}	1.1058	0.841825	2.2204×10^{-10}	2.0000	220.77000
FFA	0.0181	75.4861	0.949916	8.5959	1.9143	189.52000
GWO	4.3206×10^{-16}	1.1224	0.832974	1.7551×10^{-9}	1.9233	217.92000
DA	2.6996×10^{-3}	1.0181	0.899220	4.8877×10^{-10}	1.0000	228.64000
SSA	0.0269	1.6612	0.863027	4.3412	1.8747	116.52000
LHSSA	2.2204×10^{-16}	36.5013	0.766241	14.1930	1.9995	0.10029

TABLE XI
ESTIMATED PARAMETERS IN FUZZY ENVIRONMENT (DD MODEL) WHEN $\alpha = 0.8$

Algorithm	R_s (Ω)	R_{sh} (Ω)	I_{ph} (A)	I_{sd1} (μA)	I_{sd2} (μA)	n_1	n_2	RMSE (mA)
PSO	2.2204×10^{-16}	100.0000	0.7426	13.238	2.220×10^{-10}	2.00	2.00	29.05
FFA	2.2204×10^{-16}	1.1034	0.8331	2.220×10^{-10}	2.220×10^{-10}	1.50	1.11	222.72
GWO	1.4317×10^{-2}	73.9081	0.7673	12.968	8.489×10^{-10}	2.00	1.43	8.66
DA	2.3572×10^{-16}	2.7496	0.6802	3.754×10^{-10}	2.818×10^{-10}	1.06	1.04	251.53
SSA	1.6169×10^{-2}	4.6353	0.8661	4.672×10^{-3}	12.827	1.54	1.97	65.54
LHSSA	2.2561×10^{-2}	65.3882	0.7539	2.024	2.220×10^{-10}	1.71	1.00	0.12

TABLE XII
ESTIMATED PARAMETERS IN FUZZY ENVIRONMENT (PV MODULE) WHEN $\alpha = 0.8$

Algorithm	R_s (Ω)	R_{sh} (Ω)	I_{ph} (A)	I_{sd} (μA)	n	RMSE (mA)
PSO	2.2204×10^{-16}	2000.0000	1.2169	6938.000	3.3448	91.95800
FFA	2.2204×10^{-16}	548.3519	1.1426	88576.000	7.3094	212.37000
GWO	2.2204×10^{-16}	905.2461	1.0513	795.350	2.3831	19.14200
DA	2.2204×10^{-16}	1659.3036	1.0943	76921.000	6.7461	194.71000
SSA	1.3802×10^{-4}	1703.3602	1.3011	38435.000	4.8604	136.25000
LHSSA	0.0220	1999.9620	1.0324	65.662	1.7777	0.49438

The proposed LHSSA is investigated on different PV models, i.e., SD, DD, and PV module models. Comprehensive results affirm that LHSSA is able to obtain highly competitive performance in comparison with other algorithms, especially in terms of quality and reliability. In future work, we will study the effect of shading on the performance of the PV

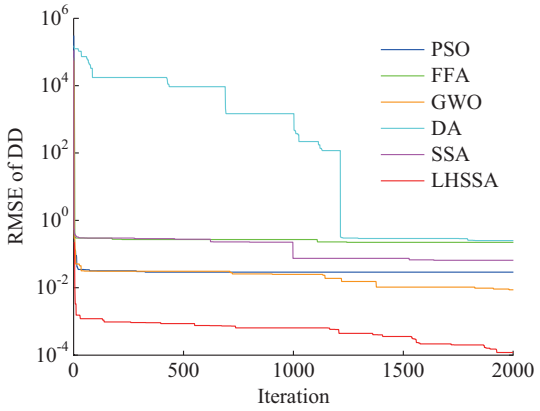

Fig. 7. Convergence curves for DD model at $\alpha = 0.8$.

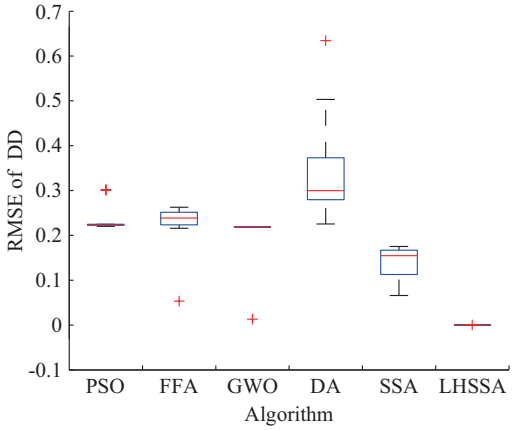

Fig. 8. Box plot for RMSE over 20 runs for DD $\alpha = 0.8$.

TABLE XIII
STATISTICAL MEASURES AMONG DIFFERENT TECHNIQUES FOR THREE MODELS UNDER FUZZY ENVIRONMENT ($\alpha = 0.8$)

Model	Algorithm	RMSE (mA)			
		Min	Mean	Max	SD
SD	PSO	220.77000	231.40000	300.55000	24.33200
	FFA	189.52000	227.43000	242.79000	146.71000
	GWO	217.92000	218.65000	219.02000	0.36142
	DA	228.64000	273.31000	295.14000	23.96100
	SSA	116.52000	161.67000	208.19000	23.10600
	LHSSA	0.10029	0.25622	0.34823	0.07818
DD	PSO	29.05000	219.53000	302.33000	74.49600
	FFA	222.72000	238.44000	251.02000	9.48900
	GWO	8.65650	118.91000	219.85000	105.79000
	DA	251.53000	11504.00000	111420.00000	35109.00000
	SSA	65.54200	137.93000	198.67000	45.38300
	LHSSA	0.11987	0.27267	391.31000	0.07176
PV module	PSO	91.95800	213.75000	276.93000	720.69000
	FFA	212.37000	246.50000	264.59000	14.30600
	GWO	19.14200	47.80500	266.10000	76.81400
	DA	194.71000	354.88000	441.70000	96.89600
	SSA	136.25000	196.20000	254.81000	51.95600
	LHSSA	0.49438	0.69770	0.90773	0.13615

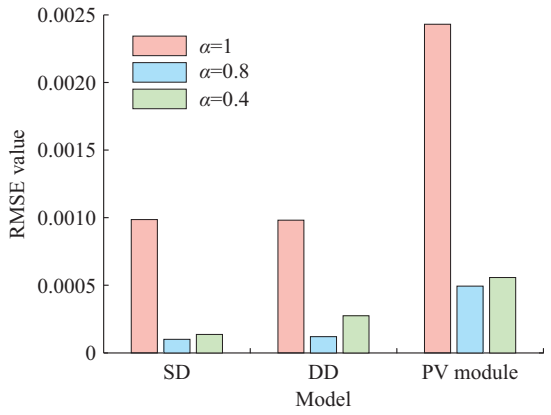

Fig. 9. Effects of α-level schemes on RMSE.

modules. Additionally, some other modification will be developed, dealing with more complex renewable energy problems and studying the use of the rough set theory for dealing with different PV models. Finally, we hope that this paper will inspire researchers in studying the uncertainty aspect of solar cell performances.

REFERENCES

[1] S. Bidyadhar and P Raseswari, "Bacterial foraging optimization approach to parameter extraction of a photovoltaic module," *IEEE Transactions on Sustainable Energy*, vol. 9, no. 1, pp. 381-389, Jan. 2018.
[2] X. Chen and K. Yu, "Hybridizing cuckoo search algorithm with biogeography-based optimization for estimating photovoltaic model parameters," *Solar Energy*, vol. 180, pp. 192-206, Mar. 2019.
[3] M. G. Villalva, J. R. Gazoli, and E. R. Filho, "Comprehensive approach to modeling and simulation of photovoltaic arrays," *IEEE Transactions on Power Electronics*, vol. 24, no. 5, pp. 1198-1208, Jun. 2009.
[4] P. Lin, S. Cheng, W. Yeh *et al*., "Parameters extraction of solar cell models using a modified simplified swarm optimization algorithm," *Solar Energy*, vol. 144, pp. 594-603, Mar. 2017.
[5] D. F. Alam, D. A. Yousri, and M. B. Eteiba, "Flower pollination algorithm based solar PV parameter estimation," *Energy Conversion and Management*, vol.101, pp. 410-422, Sept. 2015.
[6] M. F. AlHajri, K. M. El-Naggar, M. R. AlRashidi *et al*., "Optimal extraction of solar cell parameters using pattern search," *Renewable Energy*, vol. 44, pp. 238-245, Aug. 2012.
[7] X. Gao, Y. Cui, J. Hu *et al*., "Lambert W-function based exact representation for double diode model of solar cells: comparison on fitness and parameter extraction," *Energy Conversion and Management*, vol. 127, pp. 443-460, Nov. 2016.
[8] A. Orioli and A. D. Gangi, "A procedure to calculate the five-parameter model of crystalline silicon photovoltaic modules on the basis of the tabular performance data," *Applied Energy*, vol. 102, pp. 1160-1177, Feb. 2013.
[9] R. M. Rizk-Allah, "Hybridizing sine cosine algorithm with multi-orthogonal search strategy for engineering design problems," *Journal of Computational Design and Engineering*, vol. 5, no. 2, pp. 249-273, Apr. 2018.
[10] R. M. Rizk-Allah, R. A. El-Sehiemy, S. Deb *et al*., "A novel fruit fly framework for multi-objective shape design of tubular linear synchronous motor," *The Journal of Supercomputing*, vol. 73, pp. 1235-1256, Mar. 2017.
[11] R. M. Rizk-Allah and A. E. Hassanien, "New binary bat algorithm for solving 0-1 knapsack problem," *Complex & Intelligent Systems*, vol. 4, no. 1, pp. 31-53, Aug. 2017.
[12] R. M. Rizk-Allah, A. E. Hassanien, E. Mohamed *et al*., "A new binary salp swarm algorithm: development and application for optimization tasks," *Neural Computing and Applications*, vol. 31, no. 5, pp.1641-1663, May 2019.
[13] M. A. Abido and K. M. Sheraz, "Seven-parameter PV model estimation using differential evolution," *Electrical Engineering*, vol. 100, no. 2, pp. 971-981, May 2017.
[14] A. Askarzadeh and A. Rezazadeh, "Artificial bee swarm optimization algorithm for parameters identification of solar cell models," *Applied Energy*, vol. 102, pp. 943-949, Feb. 2013.
[15] N. Rajasekar, N. K. Kumar, and R. Venugopalan, "Bacterial foraging algorithm based solar PV parameter estimation," *Solar Energy*, vol. 97, pp. 255-265, Nov. 2013.
[16] A. Askarzadeh and L. D. S. Coelho, "Determination of photovoltaic modules parameters at different operating conditions using a novel bird mating optimizer approach," *Energy Conversion and Management*, vol. 89, pp. 608-614, Jan. 2015.
[17] J. Ma, Z. Bi, T. O. Ting *et al*., "Comparative performance on photovoltaic model parameter identification via bio-inspired algorithms," *Solar Energy*, vol. 132, pp. 606-616, Jul. 2016.
[18] X. Chen, K. Yu, W. Du *et al*., "Parameters identification of solar cell models using generalized oppositional teaching learning based optimization," *Energy*, vol. 99, pp. 170-180, Mar. 2016.
[19] S. Mirjalili, H. G. Amir, Z. M. Seyedeh *et al*., "Salp swarm algorithm: a bio-inspired optimizer for engineering design problems," *Advances in Engineering Software*, vol. 114, pp. 163-191, Dec. 2017.
[20] C. Kahraman, *Fuzzy Multi-criteria Decision Making: Theory and Applications with Recent Developments*. Heidelberg: Springer Science & Business Media, 2008.
[21] R. C. Eberhart and J. Kennedy, "A new optimizer using particle swarm theory," in *Proceedings of the 6th International Symposium on Micro Machine and Human Science*, Nagoya, Japan, Oct. 1995, pp. 39-43.
[22] A. E. Hassanien, R. M. Rizk-Allah, and E. Mohamed. (2018, Jun.). A hybrid crow search algorithm based on rough searching scheme for solving engineering optimization problems. *Journal of Ambient Intelligence and Humanized Computing*. [Online]. Available: https://link.springer.com/article/10.1007/s12652-018-0924-y
[23] K. Yu, J. Liang, B. Qu *et al*., "Parameters identification of photovoltaic models using an improved JAYA optimization algorithm," *Energy Conversion and Management*, vol. 150, pp. 742-753, Oct. 2017.
[24] K. Hussain, S. M. N. Mohd, S. Cheng *et al*., 'Metaheuristic research: a comprehensive survey," *Artificial Intelligence Review*, vol. 150, pp. 742-753, Oct. 2017.

Rizk Masoud Rizk-Allah received his Ph.D. degree in engineering mathematics from Menoufia University, Shebin El-Kom, Egypt. He is currently an Associate Professor at the Faculty of Engineering, Menoufia University. His research interests include multi-objective optimization, rough set theory, and the application of meta-heuristic optimization (artificial intelligence) techniques in computational engineering, renewable energy technologies and operations research problems.

Aboul Ella Hassanein is the Founder and Head of the Egyptian Scientific Research Group (SRGE) and a Professor of Information Technology at the Faculty of Computer and Artificial Intelligence, Cairo University, Cairo, Egypt. He has more than 1000 scientific research papers published in prestigious international journals and over 45 books covering such diverse topics as data mining, medical images, intelligent systems, social networks and smart environment. His other research areas include computational intelligence, medical image analysis, space sciences and telemetry mining.